Hindawi Publishing Corporation
Journal of Nanomaterials
Volume 2012, Article ID 491051, 8 pages
doi:10.1155/2012/491051

Research Article

Synthesis of Thermochromic W-Doped VO_2 (M/R) Nanopowders by a Simple Solution-Based Process

Lihua Chen,[1,2] Chunming Huang,[1] Gang Xu,[1] Lei Miao,[1] Jifu Shi,[1] Jianhua Zhou,[1] and Xiudi Xiao[1]

[1] *Key Laboratory of Renewable Energy and Gas Hydrate, Guangzhou Institute of Energy Conversion, CAS, Guangzhou 510640, China*
[2] *Graduate University of CAS, Beijing 100080, China*

Correspondence should be addressed to Gang Xu, xugang@ms.giec.ac.cn

Received 15 May 2012; Accepted 1 June 2012

Academic Editor: Vo-Van Truong

Thermochromic W-doped VO_2 nanopowders were prepared by a novel and simple solution-based method and characterized by a variety of techniques. We mainly investigated the effect of tungsten dopant on the structural properties and phase transition of $V_{1-x}W_xO_2$. The as-obtained nanopowders with tungsten content of ≤2.5 at% can be readily indexed as monoclinic VO_2 (M) while that of 3 at% assigned into the rutile VO_2 (R). The valence state of tungsten in the nanopowders is +6. TEM and XRD results show that the substitution of W atom for V in VO_2 results in a decrease of the *d* space of the (011) plane. The phase transition temperature is determined by differential scanning calorimetry (DSC). It is found, for the first time, that the reduction of transition temperature reaches to 17 K per 1 at% of W doping with the tungsten extents of ≤1 at%, but only 9.5 K per 1 at% with the tungsten extents of >1 at%. The reason of this arises from the difficulty of the formation of V^{3+}-W^{4+} and V^{3+}-W^{6+} pairs by the increasing of W ions doping in the $V_{1-x}W_xO_2$ system.

1. Introduction

Vanadium oxides have nearly 15–20 stable phases, meanwhile metalinsulator transition (MIT) has been reported in at least 8 vanadium oxide compounds (V_2O_3, VO_2, V_3O_5, V_4O_7, V_5O_9, V_6O_{11}, V_2O_5, V_6O_{13}, etc.) at temperatures ranging from −147°C to 68°C [1–3], in which VO_2 materials show the fully reversible phase transition between monoclinic VO_2 (M) and tetragonal rutile phase VO_2 (R) fascinatingly around 68°C. As a result, the resistance has a sharp change of 4–5 orders of magnitude, and the optical transmission alters correspondingly. Below the critical temperature (T_c), VO_2 is in the semiconductive state, in which the energy gap is around 0.6 eV [4], permitting high infrared (IR) transmission. Above T_c, VO_2 is in the metallic state, in which overlap between the Fermi level and the V_{3d} band eliminates the aforementioned band gap, causing vanadium dioxide to be highly reflecting or opaque in the near-infrared (NIR) region [5–8]. Furthermore, the phase transition temperature can be adjusted to near room temperature by doping, which is realized by the incorporation of metal ions into the VO_2 lattice [3]. Tungsten, molybdenum, chromium, titanium, fluorine, and niobium, and so forth are frequently used for this purpose because they produce relatively larger T_c shifts with less dopant concentrations. It has been found that tungsten might be the most effective element [9–14]. Therefore, with such properties, VO_2 materials can be considered as a promising candidate for a variety of potential applications such as energy-efficient window coatings [8], thermal sensors [15], cathode materials for reversible lithium batteries [16], electrical and infrared light switching device [17, 18].

So far, as an intelligent window material, the study of W-doped VO_2 mainly focused on thin films and nanoparticles. It has been prepared by a variety of methods involving excimer-laser-assisted metal organic deposition (ELAMOD) [19], magnetron sputtering [20], chemical vapor deposition (CVD) [21], pulsed laser deposition (PLD) [22], and vacuum evaporation [23]. However, all of these methods are not suitable for putting into practice because of complex control parameters, unstable technology, and the necessity of special and expensive equipment [24]. Chemical solution deposition

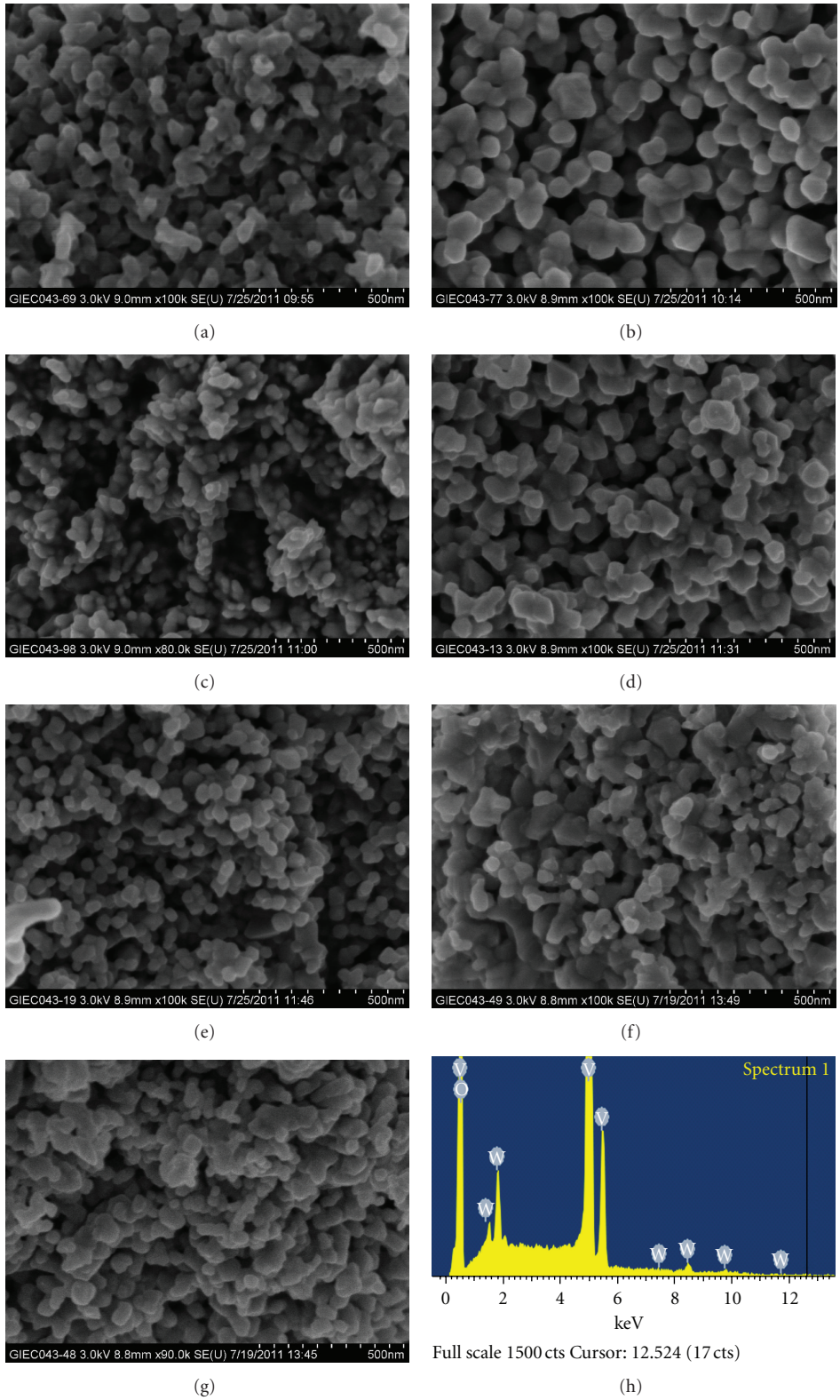

Figure 1: SEM images of vanadium dioxide nanopowders with different W-doped concentration from 0 to 3 atom% (at the intervals of 0.5) (a–g). EDS pattern for 2 at% W-doped VO_2 (h).

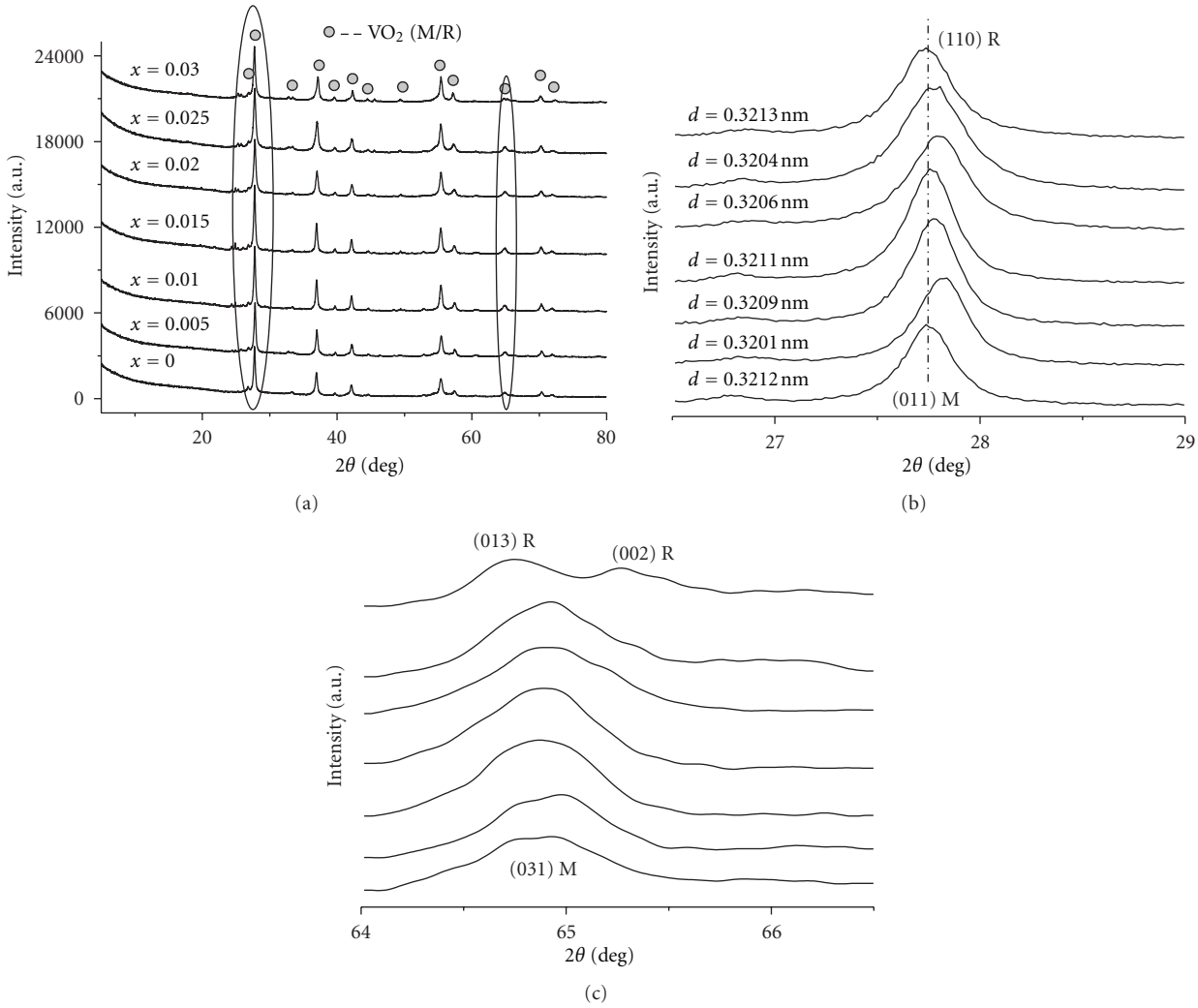

FIGURE 2: XRD patterns of $V_{1-x}W_xO_2$ nanopowders annealing at 500°C for 8 h with molar ratio of 2 : 3 (a) adding different extents of tungsten doping. A magnified version of the XRD data depicted in (b) in the $26.5° \leq 2\theta \leq 29°$ range and in (c) in the $64° \leq 2\theta \leq 66°$ range.

seems to be an alternative solution to the above problems due to its low cost and the option of metal doping. But this method usually requires specific raw materials or pretreatments which limit their practical applications [6]. Up to now, other modified methods for synthesis of M- or R-phase vanadium dioxide have been presented such as hydrothermal processes [25] and reduction-hydrolysis methods [26]. Nevertheless, long reaction time (12 h to several days) is often needed, or virulent precursor such as V_2O_5 is always required. Thus, more simple method for preparing vanadium dioxide with MIT property needs to be developed to promote its practical applications.

In this paper, we report a simple solution-based process to prepare pure VO_2 and W-doped VO_2 nanopowders with cheap and nontoxic vanadium (V) precursors and short reaction times. The characterization of the obtained nanopowders is studied through a variety of techniques. Furthermore, doping with tungsten could adjust the phase transition temperature remarkably, and thus put the thermochromic application into practice.

2. Experimental Section

2.1. Preparation of V_{1-x} W_xO_2 Nanopowders. First, a 0.5 g portion of ammonium metavanadate powders (NH_4VO_3, 99%, Tianjin Fuchen Chemical Reagents Factory) and appropriate amount of ammonium tungstate ($N_5H_{37}W_6O_{24}\cdot H_2O$, 85–90%, Sinopharm Chemical Reagent Co, Ltd.) with different W/V atom ratios were dissolved in 50 mL deionized water, respectively. Then oxalic acid dihydrate ($C_2H_2O_4\cdot 2H_2O$, 99.5%, Guangzhou Chemical Reagent Factory) was added to the above solution, where the molar ratio of NH_4VO_3 and $C_2H_2O_4\cdot 2H_2O$ was kept at 2 : 3. The mixture was stirred continuously for 30 min to form a sky blue clear solution, which indicated that the valence of vanadium in the solution was V^{4+}. As is known, the solution of V^{5+} is yellow, V^{4+} is blue, and that of V^{3+} is green, respectively. Then the above solution was dried below 100°C. Finally, W-doped VO_2 products, denoting as $V_{1-x}W_xO_2$ (x was appointed a delegate to the atomic ratio of W/V in the reactive precursors, $0 \leq x \leq 0.03$, at intervals of 0.005), were obtained after

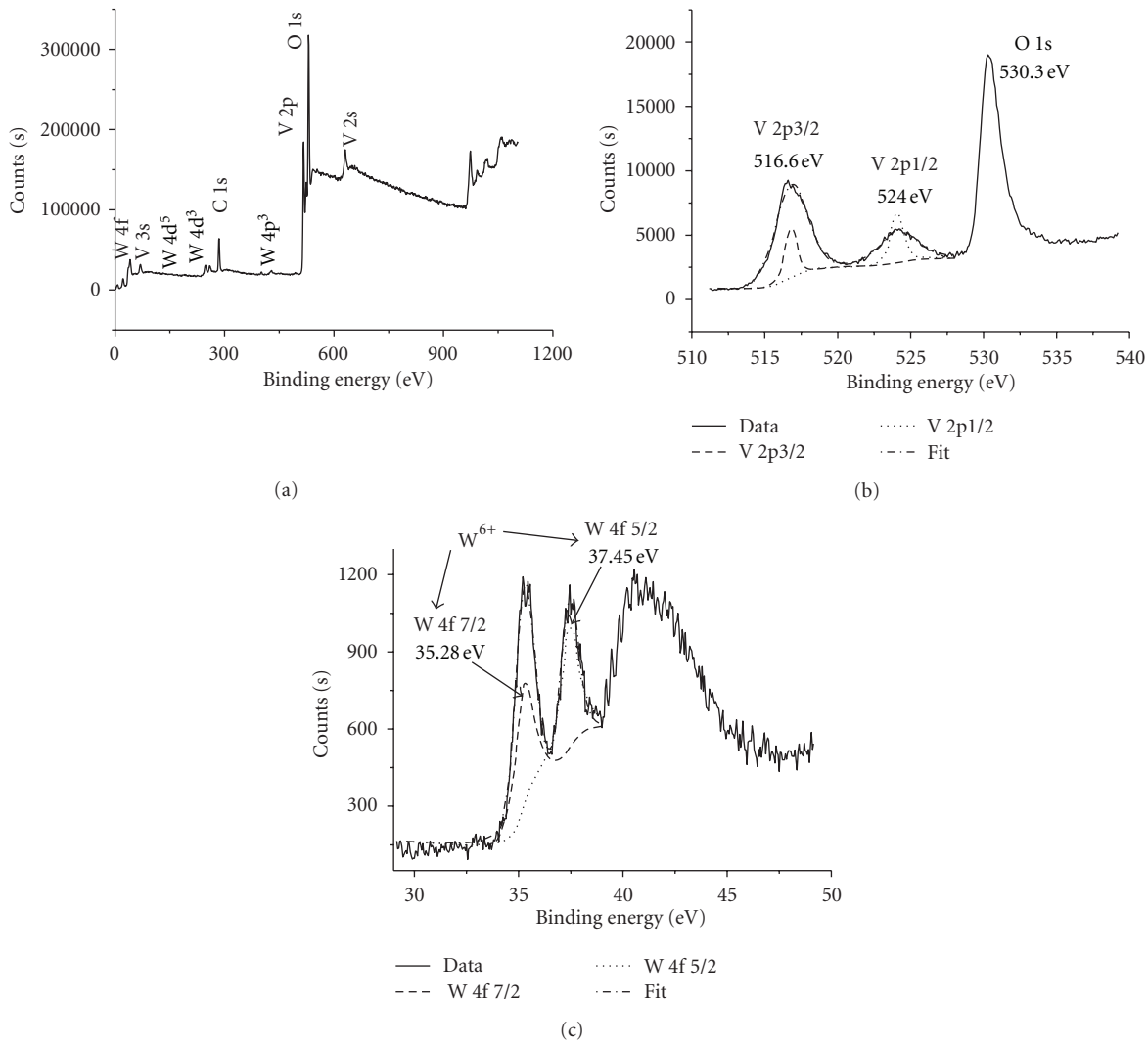

Figure 3: (a) XPS survey spectrum of 2 atom% W-doped VO_2. (b) V_{2p} peaks of the sample. (c) W_{4f} peaks of the sample.

annealing the collected powders at 500°C for 8 hours in nitrogen atmosphere. The possible reactions in the solution and the decomposition of the intermediate are listed as follows [27, 28]:

$$2NH_4VO_3 + 4C_2H_2O_4 \longrightarrow (NH_4)_2[(VO)_2(C_2O_4)_3] + 2CO_2 + 4H_2O \quad (1)$$

$$(NH_4)_2[(VO)_2(C_2O_4)_3] \longrightarrow 2VOC_2O_4 + 2NH_3 + CO + CO_2 + H_2O \quad (2)$$

$$VOC_2O_4 \longrightarrow VO_2 + CO + CO_2. \quad (3)$$

2.2. Characterization. Powder X-ray diffraction (XRD, PANalytical B.V., X′Pert Pro MPS PW3040/60) patterns of the samples were recorded in the scanning range of 5–80° at room temperature of 25°C. The morphologies, dimensions, elemental composition, and crystallinity of the nanopowders were examined by scanning electron microscopy (SEM, Hitachi, S-4800), energy dispersive X-ray spectroscopy (EDS) attached to the SEM, transmission electron microscopy (TEM), and high-resolution TEM (JEOL, JEM-2010HR), respectively. Samples for TEM observation were prepared by dispersing in ethanol. Differential scanning calorimetry (DSC, Netzsch-Bruker, STA449F3Jupiter-TENSOR27) experiments were performed using a DuPont differential thermal analyzer under atmosphere flow in the range of 25–120°C with a heating rate of $5\,K\,min^{-1}$, and in the measure procedure heating process alternates with cooling process. The valance state of the as-obtained $V_{1-x}W_xO_2$ nanopowders was characterized by means of X-ray photoelectron spectroscopy (XPS, Thermo-V-G Scientific, ESCALAB250).

3. Results and Discussion

The morphology of the undoped and W-doped VO_2 nanopowders is characterized by SEM as shown in Figure 1. It is observed in Figures 1(a) to 1(g) that the tungsten dopant

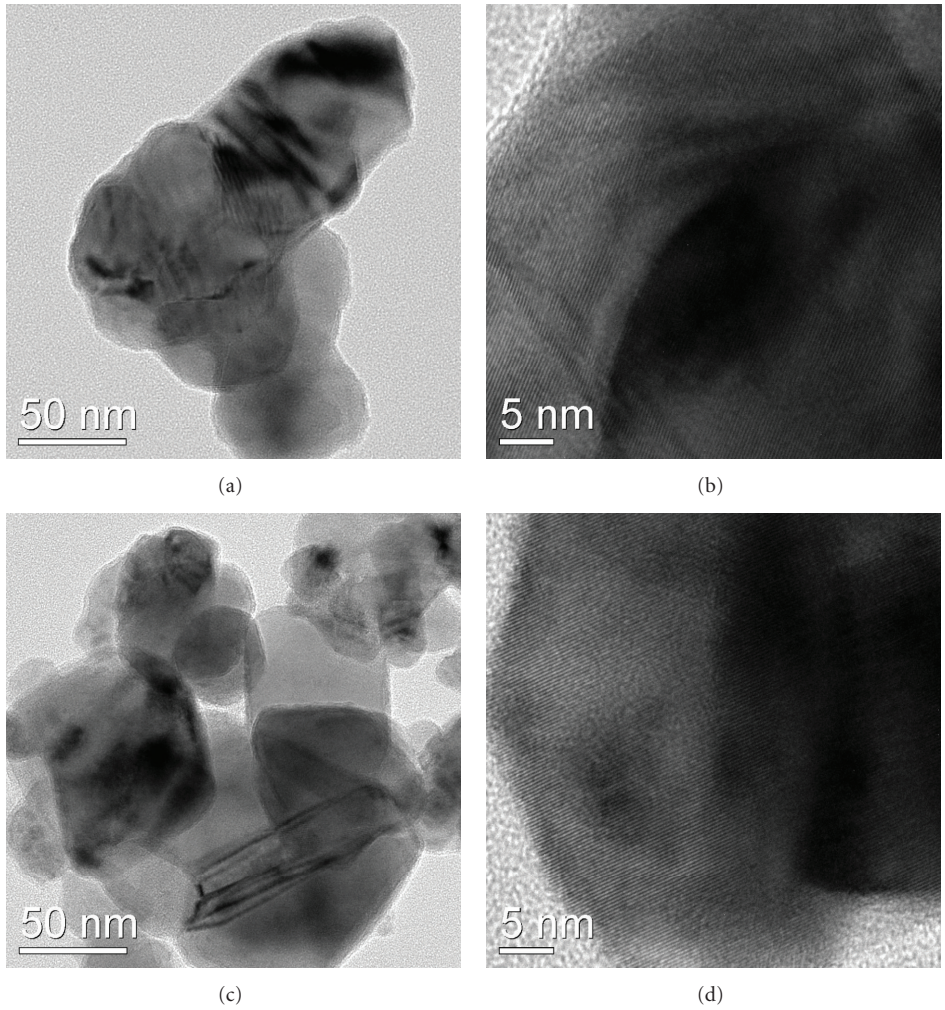

Figure 4: TEM and HRTEM images for the as-obtained undoped VO_2 (a; b) and $V_{0.98}W_{0.02}O_2$ (c; d) nanopowders.

concentration almost has no effect on the morphology of the nanoparticles, and the particle sizes are about 20–60 nm. The experimental results also indicate that particles will be congregated with the increase of annealing time. Especially, the particles with 2 at% W-doped are relatively uniform, and the size is about 25 nm, which is in favor of the practice application on thermochromic window coatings. As is known, small and uniform particles are relatively easy to disperse in solvent and obtain homogeneous coating. Therefore, the 2 at% W-doped sample is investigated in detail in the following experiments. EDS analysis results further confirm the existence of V, W, and O elements. The representative peaks of V and O elements appear in all of the obtained samples, and the representative peaks of W element also appear in each of W-doped products, which confirm a successful doping of W into VO_2. Here we just give the EDS pattern of 2 at% W-doped sample (Figure 1(h)) as a representative example.

The XRD patterns of W-doped VO_2 nanopowders with various tungsten contents are recorded in Figure 2(a). The magnified versions of the XRD data in the range of $26.5^\circ \leq 2\theta \leq 29^\circ$ and $64^\circ \leq 2\theta \leq 66^\circ$ are depicted in Figure 2(b) and Figure 2(c), respectively. It is found that the as-obtained samples with the tungsten extents of ≤2.5 at% can be readily indexed as monoclinic VO_2 (M) (JCPDS card number 79-1655), while that of 3 at% assigned into the rutile VO_2 (R) (JCPDS card number 43-1051). For the sample doped 3 at% tungsten, the peak in $26.5^\circ \leq 2\theta \leq 29^\circ$ shifts left than the others figuring out the change of VO_2 (M) (011) to VO_2 (R) (110) in Figure 2(b), and meanwhile the VO_2 (M) (310) peak splits into the VO_2 (R) (013) and (002) in $64^\circ \leq 2\theta \leq 66^\circ$ (Figure 2(c)). The above two phenomena together indicate the occurrence of the diagnostic feature for the structural phase transition from monoclinic to tetragonal VO_2 phase, which are in good agreement with previous reports [7, 29]. Therefore, the changes in peak positions of as-obtained samples indicate that an appropriate amount of tungsten doping can promote the phase transition [30].

In Figure 3, XPS analysis of the as-obtained nanopowders with 2 at% W-doped is performed to understand in detail the valance state. The spectra indicate that there are four elements: oxygen, vanadium, carbon, and tungsten with binding energy peaks corresponding to C1s, O1s, V2s, V2p, V3s, W4f, W4d, and W4p in W-doped VO_2 nanopowders

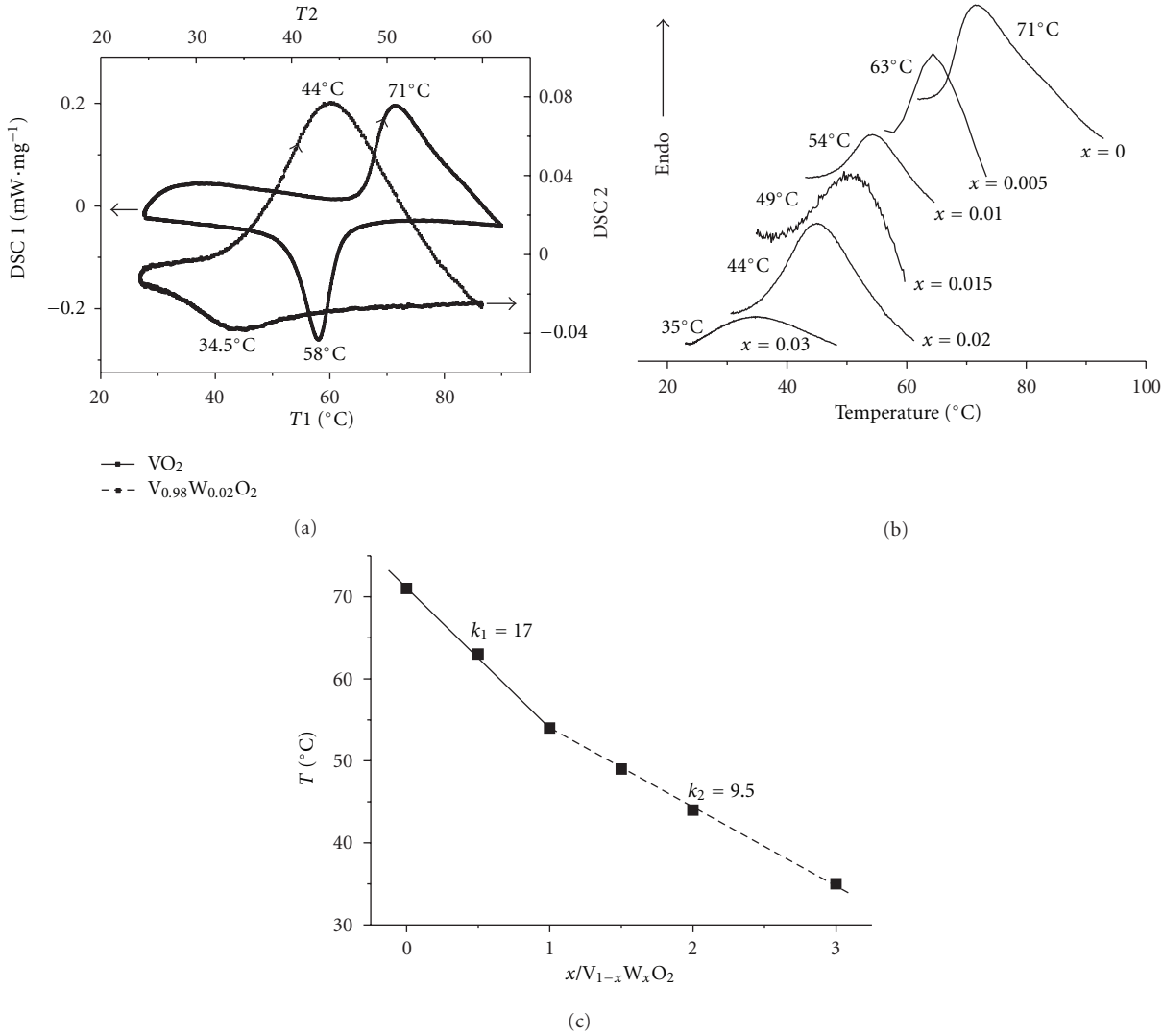

FIGURE 5: DSC curves of undoped VO_2 and 2 atom% W-doped VO_2 nanopowders during the heating and cooling cycles (a). The curves of as-obtained samples ($V_{1-x}W_xO_2$, x = 0–0.03, at intervals of 0.005) upon heating process (b). Effect of tungsten-doped vanadium dioxide concentration on the phase transition temperature upon heating process (c).

(Figure 3(a)). The forms of carbon are possibly from surface contamination [5, 9, 30]. The data reveals that the peak at 530.3 eV is associated with O1s [26]. The peaks located at 516.6 eV (reported values: 515.7–516.6 eV [5, 6, 9, 26, 30, 31]) and 524.0 eV (reported values: 522.6–524.0 eV [5, 6, 9, 26, 29, 30]) correspond to $V_{2p3/2}$ and $V_{2p1/2}$ (Figure 3(b)), respectively, and the binding energy of $V_{2p3/2}$ increases slightly after W doping [30]. The W_{4f} peaks follow with binding energies of $W_{4f7/2}$ and $W_{4f5/2}$ at 35.28 eV and 37.45 eV, respectively. According to the standard binding energy, tungsten atoms in these nanopowders exist as W^{6+} (Figure 3(c)) [9]. N-type semiconductor could form as W^{6+} ions replace V^{4+} ions.

TEM images of the undoped VO_2 and 2 at% W-doped VO_2 nanopowders are shown in Figures 4(a) and 4(c). The morphologies and sizes of the as-obtained samples are consistent with those of SEM images in Figures 1(a) and 1(e). Figures 4(b) and 4(d) show the lattice-resolved HRTEM images. The fringe spacing is 0.321 nm for undoped VO_2 (Figure 4(b)) sample, which is consistent with the d space of the (011) plane of monoclinic VO_2 (M) phase [32, 33], and the fringe spacing reduces to 0.314 nm (Figure 4(d)) for the sample of 2 at% W-doped VO_2. This decreased tendency of the fringe spacing with W doping is consistent with the calculated results by Scherrer formula. As the radius of W^{6+} ion (60 pm [34]) is smaller than that of the V^{4+} ion about 63 pm. The interstitial W^{6+} ions will cause the atoms to have larger interatomic spacings, and the interatomic spacings will be reduced in the case of substitutional defects with W^{6+} ions. The TEM results suggest that the substitution of W^{6+} ions for V^{4+} plays a dominant role in this work, which results in the reduction of d_{011} spacing. As the tungsten dopant concentration is 2 at%, the (011) peak of monoclinic VO_2 (M) shifts from 27.74° (undoped VO_2) to 27.79°, indicating the decrease of the crystal lattice spacing according to the Bragg equation ($2d\sin\theta = \lambda$; $\lambda_{Cu} = 0.154$ nm) [29, 35, 36].

As regards the rule of substitution or interstitial of W^{6+} ions for V^{4+} is unknown, and it needs further research.

When the phase transition of VO_2 occurs, it exhibits a noticeable endothermal or exothermal profile in the DSC curve. Figure 5(a) shows the typical DSC curves of undoped and 2 at% W-doped VO_2 nanopowders. With 2 at% W-doped sample, Mott phase transition arises at around 44°C and 34.5°C for the heating and cooling cycles, compared to 71°C and 58°C for the undoped VO_2, respectively. The phase transition can be modified under the different factors such as defect density or lattice change [3, 29]. The appearance of endothermal and exothermal peaks during the heating and cooling process confirms the first-order transition between monoclinic VO_2 (M) and tetragonal rutile VO_2 (R) [7]. To be vital for the practical thermochromic effect applications, the phase transition temperature of W-doped must be approaching to room temperature. In this case, the phase transition temperature could be reduced to 35°C with 3 at% W-doped in Figure 5(b).

A nonlinear decrease of the phase transition temperature with increasing percent of tungsten atom incorporation is observed upon heating process (Figure 5(c)). And the nonlinear decrease can be described by two linear fits. The reduction of transition temperature is estimated to be about 17 K per 1 at% of W doping with the tungsten extents of ≤1 at%, but only 9.5 K per 1 at% with the tungsten extents of >1 at%. With tungsten ion doping into VO_2, the reaction takes place as follows: $2V^{4+} + W^{4+} \rightarrow 2V^{3+} + W^{6+}$, which results in the formation of V^{3+}-V^{4+} and V^{3+}-W^{6+} pairs [35]. Then the transition temperature will be reduced due to the loss of direct bonding between V ions, which is resulted from the forming of the pairs. We can now assume that the change of transition temperature is determined by the difficulty of initial formation of V^{3+}-V^{4+} and V^{3+}-W^{6+} pairs. At the beginning, the pairs form easily with lower tungsten dopant concentration, so the transition temperature could remarkably change. By following the increase of W ions, it becomes relatively difficult to form the V^{3+}-V^{4+} and V^{3+}-W^{6+} pairs right away, resulting in a more gradual change in the transition temperature.

4. Conclusions

Well-crystallized nanopowders of W-doped VO_2 (M/R) were successfully synthesized by a simple solution-based process through the reaction of ammonium metavanadate (NH_4VO_3) and oxalic acid dihydrate ($C_2H_2O_4 \cdot 2H_2O$) followed by adding to appropriate ammonium tungstate ($N_5H_{37}W_6O_{24} \cdot H_2O$). It is shown that tungsten dopant concentration almost has no effect on the morphology of the nanoparticles and the granular particles are about 20–60 nm. As-obtained nanopowders with the tungsten extents of ≤2.5 at% can be readily indexed as monoclinic VO_2 (M), while that of 3 at% assigned into the rutile VO_2 (R). Substitutional W^{6+} ions could reduce the interatomic spacings, which results in the decrease of the *d* space of the (011) plane in monoclinic VO_2 (M) phase. Moreover, we found that the difficulty level in initial formation of V^{3+}-V^{4+} and V^{3+}-W^{6+} pairs determines the rate of change of the critical temperature. The reduction of transition temperature is estimated to be about 17 K per 1 at% of W doping with the tungsten extents of ≤1 at%, only about 9.5 K per 1 at% with the tungsten extents of >1 at%. With 3 at% W-doped VO_2, the phase transition temperature can be reduced to 35°C. In short, this paper provides a simple solution-based method to prepare W-doped VO_2 nanopowders with good thermochromic properties showing the transition temperature required to building glazing, which is in favor of promoting the practical applications of smart window.

Acknowledgments

This work is supported by the National Natural Science Foundation of China (no. 51102235) and National Science Foundation of Guangdong Province (no. 9451007006004079).

References

[1] F. J. Morin, "Oxides which show a metal-to-insulator transition at the neel temperature," *Physical Review Letters*, vol. 3, no. 1, pp. 34–36, 1959.

[2] D. P. Partlow, S. R. Gurkovich, K. C. Radford, and L. J. Denes, "Switchable vanadium oxide films by a sol-gel process," *Journal of Applied Physics*, vol. 70, no. 1, pp. 443–452, 1991.

[3] Z. F. Peng, Y. Wang, Y. Y. Du, D. Lu, and D. Z. Sun, "Phase transition and IR properties of tungsten-doped vanadium dioxide nanopowders," *Journal of Alloys and Compounds*, vol. 480, no. 2, pp. 537–540, 2009.

[4] G. H. Liu, X. Y. Deng, and R. Wen, "Electronic and optical properties of monoclinic and rutile vanadium dioxide," *Journal of Materials Science*, vol. 45, no. 12, pp. 3270–3275, 2010.

[5] J. Zhang, Eerdemutu, C. X. Yang et al., "Size- and shape-controlled synthesis of monodisperse vanadium dioxide nanocrystals," *Journal of Nanoscience and Nanotechnology*, vol. 10, no. 3, pp. 2092–2098, 2010.

[6] Z. T. Zhang, Y. F. Gao, Z. Chen et al., "Thermochromic VO_2 thin films: solution-based processing, improved optical properties, and lowered phase transformation temperature," *Langmuir*, vol. 26, no. 13, pp. 10738–10744, 2010.

[7] C. Z. Wu, X. D. Zhang, J. Dai et al., "Direct hydrothermal synthesis of monoclinic VO_2(M) single-domain nanorods on large scale displaying magnetocaloric effect," *Journal of Materials Chemistry*, vol. 21, no. 12, pp. 4509–4517, 2011.

[8] G. Xu, C. M. Huang, P. Jin, M. Tazawa, and D. M. Chen, "Nano-Ag on vanadium dioxide. I. Localized spectrum tailoring," *Journal of Applied Physics*, vol. 104, no. 5, Article ID 053101, 6 pages, 2008.

[9] J. W. Ye, L. Zhou, F. J. Liu et al., "Preparation, characterization and properties of thermochromic tungsten-doped vanadium dioxide by thermal reduction and annealing," *Journal of Alloys and Compounds*, vol. 504, no. 2, pp. 503–507, 2010.

[10] J. Z. Yan, Y. Zhang, W. X. Huang, and M. J. Tu, "Effect of Mo-W Co-doping on semiconductor-metal phase transition temperature of vanadium dioxide film," *Thin Solid Films*, vol. 516, no. 23, pp. 8554–8558, 2008.

[11] C. Batista, V. Teixeira, and R. M. Ribeiro, "Synthesis and characterization of $V_{1-x}Mo_xO_2$ thermochromic coatings with

reduced transition temperatures," *Journal of Nanoscience and Nanotechnology*, vol. 10, no. 2, pp. 1393–1397, 2010.

[12] W. Burkhardt, T. Christmann, S. Franke et al., "Tungsten and fluorine co-doping of VO_2 films," *Thin Solid Films*, vol. 402, no. 1-2, pp. 226–231, 2002.

[13] I. Takahashi, M. Hibino, and T. Kudo, "Thermochromic properties of double-doped VO_2 thin films prepared by a wet coating method using polyvanadate-based sols containing W and Mo or W and Ti," *Japanese Journal of Applied Physics*, vol. 40, no. 3, pp. 1391–1395, 2001.

[14] C. Marini, E. Arcangeletti, D. D. Castro et al., "Optical properties of $V_{1-x}Cr_xO_2$ compounds under high pressure," *Physical Review B*, vol. 77, no. 23, Article ID 235111, 9 pages, 2008.

[15] C. Sella, M. Maaza, O. Nemraoui, J. Lafait, N. Renard, and Y. Sampeur, "Preparation, characterization and properties of sputtered electrochromic and thermochromic devices," *Surface and Coatings Technology*, vol. 98, no. 1–3, pp. 1477–1482, 1998.

[16] J. Ni, W. T. Jiang, K. Yu, Y. F. Gao, and Z. Q. Zhu, "Hydrothermal synthesis of VO_2 (B) nanostructures and application in aqueous Li-ion battery," *Electrochim Acta*, vol. 56, no. 5, pp. 2122–2126, 2011.

[17] C. H. Chen, R. F. Wang, L. Shang, and C. F. Guo, "Gate-field-induced phase transitions in VO_2: monoclinic metal phase separation and switchable infrared reflections," *Applied Physics Letters*, vol. 93, no. 17, Article ID 171101, 3 pages, 2008.

[18] B. Viswanath, C. Ko, and S. Ramanathan, "Thermoelastic switching with controlled actuation in VO_2 thin films," *Scripta Materialia*, vol. 64, no. 6, pp. 490–493, 2011.

[19] M. Nishikawa, T. Nakajima, T. Kumagai, T. Okutani, and T. Tsuchiya, "Ti-doped VO_2 films grown on glass substrates by excimer-laser-assisted metal organic deposition process," *Japanese Journal of Applied Physics*, vol. 50, no. 1, pp. 01BE04–01BE04-5, 2011.

[20] G. Gopalakrishnan and S. Ramanathan, "Compositional and metal-insulator transition characteristics of sputtered vanadium oxide thin films on yttria-stabilized zirconia," *Journal of Materials Science*, vol. 46, no. 17, pp. 5768–5774, 2011.

[21] R. Binions, G. Hyett, C. Piccirillo, and I. P. Parkin, "Doped and un-doped vanadium dioxide thin films prepared by atmospheric pressure chemical vapour deposition from vanadyl acetylacetonate and tungsten hexachloride: the effects of thickness and crystallographic orientation on thermochromic properties," *Journal of Materials Chemistry*, vol. 17, no. 44, pp. 4652–4660, 2007.

[22] R. T. R. Kumar, B. Karunagaran, D. Mangalaraj, S. K. Narayandass, P. Manoravi, and M. Joseph, "Characteristics of amorphous VO_2 thin films prepared by pulsed laser deposition," *Journal of Materials Science*, vol. 39, no. 8, pp. 2869–2871, 2004.

[23] F. C. Case, "Modifications in the phase transition properties of predeposited VO_2 films," *Journal of Vacuum Science & Technology A*, vol. 2, no. 4, p. 1509, 1984.

[24] Z. F. Peng, W. Jiang, and H. Liu, "Synthesis and electrical properties of tungsten-doped vanadium dioxide nanopowders by thermolysis," *The Journal of Physical Chemistry C*, vol. 111, no. 3, pp. 1119–1122, 2007.

[25] J. Li, C. Y. Liu, and L. J. Mao, "The character of W-doped one-dimensional VO_2 (M)," *Journal of Solid State Chemistry*, vol. 182, no. 10, pp. 2835–2839, 2009.

[26] C. L. Xu, L. Ma, X. Liu, W. Y. Qiu, and Z. X. Su, "A novel reduction–hydrolysis method of preparing VO_2 nanopowders," *Materials Research Bulletin*, vol. 39, no. 7-8, pp. 881–886, 2004.

[27] D. N. Sathyanarayana and C. C. Patel, "Studies of ammonium dioxovanadium(V) bisoxalate dihydrate," *Bulletin of the Chemical Society of Japan*, vol. 37, no. 12, pp. 1736–1740, 1964.

[28] D. N. Sathyanarayana and C. C. Patel, "Studies on oxovanadium (IV) oxalate hydrates," *Journal of Inorganic and Nuclear Chemistry*, vol. 27, no. 2, pp. 297–302, 1965.

[29] L. Whittaker, T. L. Wu, C. J. Patridge, G. Sambandamurthy, and S. Banerjee, "Distinctive finite size effects on the phase diagram and metal-insulator transitions of tungsten-doped vanadium(iv) oxide," *Journal of Materials Chemistry*, vol. 21, no. 15, pp. 5580–5592, 2011.

[30] C. X. Cao, Y. F. Gao, and H. J. Luo, "Pure single-crystal rutile vanadium dioxide powders: synthesis, mechanism and phase-transformation property," *Journal of Physical Chemistry C*, vol. 112, no. 48, pp. 18810–18814, 2008.

[31] N. Alov, D. Kutsko, I. Spirovová, and Z. Bastl, "XPS study of vanadium surface oxidation by oxygen ion bombardment," *Surface Science*, vol. 600, no. 8, pp. 1628–1631, 2006.

[32] L. Whittaker, C. Jaye, Z. G. Fu, D. A. Fischer, and S. Banerjee, "Depressed phase transition in solution-grown VO_2 nanostructures," *Journal of the American Chemical Society*, vol. 131, no. 25, pp. 8884–8894, 2009.

[33] H. H. Yin, M. Luo, K. Yu et al., "Fabrication and temperature-dependent field-emission properties of bundlelike VO_2 nanostructures," *ACS Applied Materials & Interfaces*, vol. 3, no. 6, pp. 2057–2062, 2011.

[34] J. T. Zeng, Y. Wang, Y. X. Li, Q. B. Yang, and Q. R. Yin, "Ferroelectric and piezoelectric properties of tungsten doped $CaBi_4Ti_4O_{15}$ ceramics," *Journal of Electroceramics*, vol. 21, no. 1–4, pp. 305–308, 2008.

[35] C. Tang, P. Gergopoulos, M. E. Fine, and J. B. Cohen, "Local atomic and electronic arrangements in $W_xV_{1-x}O_2$," *Physical Review B*, vol. 31, no. 2, pp. 1000–1011, 1985.

[36] L. Whittaker, C. J. Patridge, and S. Banerjee, "Microscopic and nanoscale perspective of the metal−insulator phase transitions of VO_2: some new twists to an old tale," *The Journal of Physical Chemistry Letters*, vol. 2, no. 7, pp. 745–758, 2011.